

# A mobile polar atmospheric parameter measurement system: II. First atmospheric turbulence observation at Antarctic Taishan Station

TIAN Qiguo<sup>1</sup>, JIANG Peng<sup>1,2\*</sup>, WU Xiaoqing<sup>3</sup>, JIN Xinmiao<sup>1</sup>, LU Shan<sup>2</sup>, JI Tuo<sup>1</sup>,  
CHAI Bo<sup>1</sup>, ZHANG Shaohua<sup>1</sup> & ZHOU Hongyan<sup>1,2</sup>

<sup>1</sup> Polar Research Institute of China, Shanghai 200136, China;

<sup>2</sup> Key Laboratory for Research in Galaxies and Cosmology, Department of Astronomy, University of Science and Technology of China, Chinese Academy of Sciences, Hefei 230026, China;

<sup>3</sup> Key Laboratory of Atmospheric Composition and Optical Radiation, Anhui Institute of Optics and Fine Mechanics, Chinese Academy of Sciences, Hefei 230031, China

Received 21 October 2014; accepted 9 February 2015

**Abstract** This is the second paper of a series devoted to atmospheric optical turbulence  $C_n^2$  observation using a mobile polar atmospheric parameter measurement system. We present the initial results of  $C_n^2$  measurement at Antarctic Taishan Station using micro-thermal sensors and a three-dimensional sonic anemometer at height  $\sim 2.0$  m above the snow surface. The site testing experiments were carried out during the 30th Chinese National Antarctic Research Expedition (CHINARE). We collected about 1 000 h of data between 30 December 2013 and 10 February 2014. The  $C_n^2$  curve exhibits clear daily structures, with two peaks around midnight and midday and two troughs around 7:30 and 17:00 local time (UTC+5). The mean  $C_n^2$  is  $2.7 \times 10^{-15} \text{ m}^{-2/3}$  and the 25th and 75th percentiles of the  $C_n^2$  cumulative distribution are  $9.6 \times 10^{-16} \text{ m}^{-2/3}$  and  $6.2 \times 10^{-15} \text{ m}^{-2/3}$ , respectively. Meteorological parameters such as temperature, relative humidity, wind speed, and air pressure are also presented.

**Keywords** micro-thermal sensors, three-dimensional sonic anemometer, turbulence, site testing, Antarctic Plateau, Kunlun Station, Taishan Station

**Citation:** Tian Q G, Jiang P, Wu X Q, et al. A mobile polar atmospheric parameter measurement system: II. First atmospheric turbulence observation at Antarctic Taishan Station. *Adv Polar Sci*, 2015, 26: 140-146, doi: 10.13679/j.advps.2015.2.00140

## 1 Introduction

“Seeing” is the most important environmental condition for optical astronomy observations. This is severely limited by atmospheric optical turbulence and generally considered as a superposition of contributions from two atmospheric layers: the surface boundary layer and free atmosphere

above. Searching for sites with superb observing conditions has become an increasingly important matter in astronomy and great efforts have been made in worldwide site testing campaigns. The Antarctic Plateau, which provides a unique environment for observational astronomy, has drawn substantial attention in recent years<sup>[1-2]</sup>. The cold, dry and stable air, high altitude, weak surface wind speed, thin boundary layer, and long continuous observations during polar nights offer observation conditions recognized as superior to any other sites on the earth.

\* Corresponding author (email: jpaty@mail.ustc.edu.cn)

Over the last two decades, great efforts have been made in campaigns of site testing in the Antarctic at four plateau sites, Amundsen-Scott South Pole Station, Concordia Station at Dome C, Kunlun Station at Dome A, and Fuji Station at Dome F. These are operated by the United States, France/Italy, China, and Japan, respectively. The South Pole Station is the first location where astronomical activities were conducted on the Antarctic Plateau. Near-Infrared sky brightness observed there by the IRPS (InfraRed Photometer-Spectrometer) showed that flux in the  $K_{\text{dark}}$  band is two orders of magnitude smaller than that at temperate observatories<sup>[3-5]</sup>. Seeing, as measured by micro-thermal sensors<sup>[6]</sup>, SODAR (Sound Detection And Ranging)<sup>[7]</sup> and DIMM (Differential Image Motion Monitor)<sup>[8]</sup>, reaches 1.8 arcsec, is similar to that at temperate sites. However, the boundary layer (as low as 200–300 m)<sup>[9-10]</sup>, isoplanatic angle and coherence time at South Pole station are superior to any of those sites. The depth of the boundary layer at South Pole is too high to consider raising a telescope above it. The katabatic wind in Antarctica starts from the highest points originally, therefore on the plateau summits, the wind speed is much reduced, leading to a significantly thinner surface boundary layer than that at the South Pole<sup>[9]</sup>. Joint observation using the MASS (Multi-Aperture Scintillation Sensor) and SODAR for experiments on seeing by J.S. Lawrence and coworkers indicated that average seeing above 30 m at Dome C was 0.27 arcsec<sup>[11]</sup>. Ground-level seeing there was 1.3 arcsec<sup>[12-13]</sup> on average, and mid-infrared sky brightness is similar to that measured at the South Pole<sup>[14]</sup>. Nevertheless, boundary layer depth at Dome C is extraordinarily thin (~36 m). Raising a telescope above the boundary layer could realize superior seeing conditions. Promising site testing results at Dome C drove astronomers to conduct site testing campaigns at Dome A, which is the highest region (elevation 4 093 m) of the Antarctic Plateau<sup>[15-16]</sup>. An exciting development is depth measurement of the boundary layer using a sonic radar as described in Bonner et al.<sup>[17]</sup>, showing that the median depth is as thin as 13.9 m, much thinner even than that at Dome C. Recently, seeing at Dome F was observed using a DIMM at height 11 m above the snow surface, and observed median seeing (0.52 arcsec) was similar to that at Dome C<sup>[18]</sup>. In addition to Kunlun Station at Dome A, a new inland station Taishan (+76°58', -73°51') was established during the 30th Chinese National Antarctic Research Expedition (CHINARE). Taishan Station is between Zhongshan and Kunlun stations at elevation 2 621 m. Easy access to Taishan Station makes astronomical activities easier to conduct. Site testing will provide key information for these activities. Seeing can be calculated by integrating  $C_n^2$  measured with height in the atmosphere. Because of the simplicity and reliability, micro-thermal sensors normally carried by balloons<sup>[10,19]</sup> or installed on towers<sup>[6]</sup> have become a commonly used probe to measure  $C_n^2$  height distributions. In 1996, Marks et al. observed the  $C_n^2$  distribution and thereby obtained seeing conditions at the South Pole<sup>[6]</sup> using a 27-m tower equipped with three pairs of micro-thermal sensors at three different levels.

In 2013, a mobile polar atmospheric parameter measurement system was designed and constructed to measure  $C_n^2$  and meteorological parameters in Antarctica<sup>[20]</sup>. It was equipped with a pair of micro-thermal sensors, three-dimensional (3D) sonic anemometer, temperature and humidity sensors, wind speed and direction sensors, barometer, and infrared thermometer. We observed  $C_n^2$  for the first time at Taishan Station using the micro-thermal sensors and 3D sonic anemometer simultaneously. This paper presents our results from the 30th CHINARE at 2013/2014 season, between 30 December 2013 and 10 February 2014. After the observation at Taishan Station, the instrument was transported to Zhongshan Station to observe  $C_n^2$  in winter for the first time, and it is planned to perform such measurements at Kunlun Station in summer during the 31st CHINARE. The observation results will provide key information for astronomical activities at Taishan, Zhongshan and Kunlun stations.

## 2 Experimental and theoretical background

Details of the mobile polar atmospheric parameter measurement system have been described elsewhere<sup>[20]</sup> and only a brief description is presented here. Figure 1 shows a photograph of the apparatus at Taishan Station, which consists of a CR5000 data logger, a pair of micro-thermal sensors, CSAT3 3D sonic anemometer, HMP155 temperature and humidity sensors, 05103V wind speed and direction sensors, SI-111 infrared radiometer, CS106 barometer, power supply system, and 3 m-high tower. The key elements of the system are the micro-thermal sensors at ~2.0 m height, which were used to observe  $C_n^2$  with the high resolution of  $\sim 3 \times 10^{-18} \text{ m}^{-2/3}$ . The CSAT3 was mounted at the same altitude,



**Figure 1** Mobile polar atmospheric parameter measurement system at Taishan Station, on January 11, 2014. Micro-thermal sensors are ~2.0 m above the snow surface.

to record  $C_n^2$  simultaneously with the low resolution of  $\sim 5 \times 10^{-16} \text{ m}^{-2/3}$ . The HMP155 and 05103V were installed at heights 0.5 m and 2.0 m, respectively. The tower was on the upwind side of Taishan Station (wind direction is generally stable),  $\sim 500$  m from the station center, so the effect of heat was minimal. The apparatus was powered by a generator at the station.

The micro-thermal sensor pair measured the temperature structure constant associated with turbulence<sup>[21]</sup>:

$$C_T^2(\bar{r}, h) = \langle [T(\bar{x}, h) - T(\bar{x} + \bar{r}, h)]^2 \rangle r^{-2/3}, \quad (1)$$

where  $\bar{r}$  is separation of the sensors and  $h$  is altitude. From the theory of Kolmogorov, with  $r$  lines between the inner and outer scales of the turbulent motion, the refractive index structure constant can be expressed as<sup>[21]</sup>

$$C_n^2(h) = \left[ 79 \times 10^{-6} \frac{P(h)}{T^2(h)} \right]^2 C_T^2(\bar{r}, h), \quad (2)$$

where  $P(h)$  and  $T(h)$  are pressure and temperature, respectively.

The diameter of the wire in the micro-thermal sensor is  $10 \mu\text{m}$ , the resistance of which can be expressed as a function of temperature  $T$ :

$$R = R_0 [1 + \alpha(T - T_0)], \quad (3)$$

where  $R_0$  is resistance at temperature  $T_0$  and  $\alpha$  is the temperature coefficient of resistance. The resistance variation of the sensors, and thus the output voltage of which is proportional to the very small and rapid temperature fluctuations associated with the turbulence, say  $\Delta R = \alpha R_0 \Delta T$  and  $\Delta V = A \Delta T$ , where  $A$  is the calibration coefficient. In this way, the connection between  $\Delta V$  and  $C_T^2$  is made. Then, data from the HMP155 and CS106 were used to translate  $C_T^2$  to  $C_n^2$  (Eq. 2).

The 3D sonic anemometer<sup>[22]</sup> is based on the Doppler effect. From measurements of transmission time of the sonic pulse along three non-orthogonal axes, wind speed and sonic sound velocity can be obtained. Since the sound velocity is a function of temperature and humidity, then the so-called ultrasonic temperature  $T_s$  can be expressed as<sup>[22]</sup>

$$T = \frac{T_s}{1 + 0.51q}, \quad (4)$$

where  $q$  is specific humidity. Since  $q$  can often be ignored,  $T_s$  can be used as temperature. In light of the Taylor assumption and observed wind speed, recorded temperature time sequences at a single point can be converted to the temperature difference between two spatially separated points. Thus,  $C_T^2$  can be written as<sup>[21,23]</sup>

$$C_T^2 = \langle [T(t) - T(t - \tau)]^2 \rangle (\bar{V}\tau)^{-2/3}, \quad (5)$$

where  $\tau$  is the time interval indicated by the average wind speed  $\bar{V}$ . Then,  $C_n^2$  can be obtained by Eq. (2).

### 3 Results

The site testing experiment was carried out by the mobile polar atmospheric parameter measurement system at Taishan Station from 30 December 2013 to 10 February 2014. The online data processing procedure recorded one measurement

data every 20 s and, for the sake of clarity, average values over 10 min are presented herein.

Figure 2 shows temperatures observed at 0.5-m and 2.0-m heights by the HMP155, along with the snow surface radiation temperature measured by the SI-111 infrared radiometer. Hour 0 in the figure corresponds to midnight 31 December 2013. Table 1 shows that maximum, minimum, and mean temperatures at 2.0 m were  $-12.2^\circ\text{C}$ ,  $-38.1^\circ\text{C}$ , and  $-22.1^\circ\text{C}$ , respectively. The temperature difference between the two levels was very small, with the difference between mean values less than  $0.1^\circ\text{C}$ . The maximum, minimum and mean snow-surface radiation temperature was  $-13.7^\circ\text{C}$ ,  $-41.8^\circ\text{C}$ , and  $-24.5^\circ\text{C}$ , respectively (Table 1). A histogram of temperature at 2.0-m height is shown in Figure 3. Also included in the figure are cumulative temperature distributions at 2.0 and 0.5 m and surface radiation temperature. The 25th, 50th and 75th percentiles of 2.0-m temperature were  $-26.1^\circ\text{C}$ ,  $-22.0^\circ\text{C}$  and  $-18.5^\circ\text{C}$ , respectively. Corresponding results are listed in Table 1.

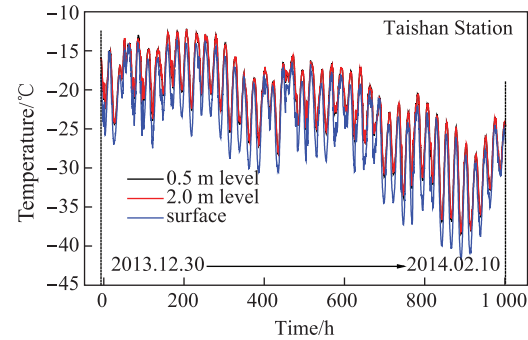


**Figure 2** Measured temperatures at Taishan Station in summer. Results at 0.5-m and 2.0-m heights and surface radiation temperature were measured by HMP155 and SI-111 sensors, respectively. Temperature differences between the two levels are very small, so black curve is almost overlaid by red one.

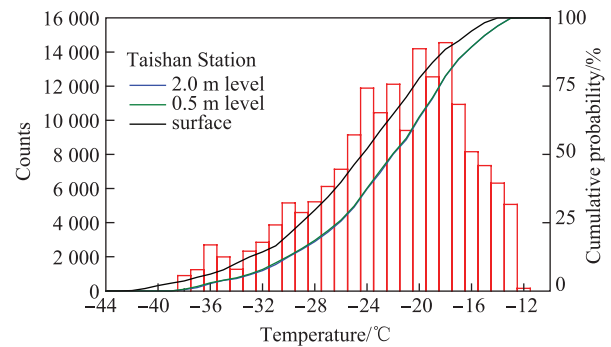


**Figure 3** Histogram of Taishan Station temperature at 2.0-m height, along with cumulative distributions of temperature at 2.0 m and 0.5 m heights and surface radiation temperature.

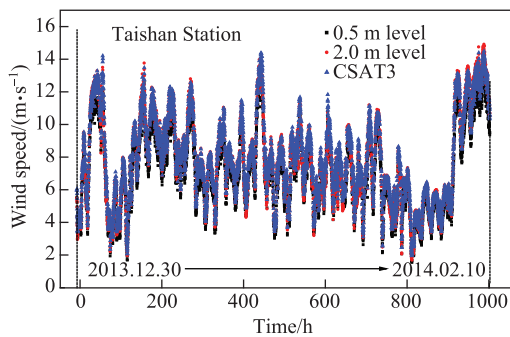
Figure 4 shows Taishan Station wind speeds at 0.5-m and 2.0-m heights observed by the 05103V and CSAT3. The 2.0-m wind speeds measured by the two sensors agree well. Maximum, minimum, and mean wind speeds from the 05103V were  $14.91$ ,  $1.68$  and  $7.73 \text{ m}\cdot\text{s}^{-1}$ , respectively. Speeds

**Table 1** Temperature and wind speeds measured at Taishan Station

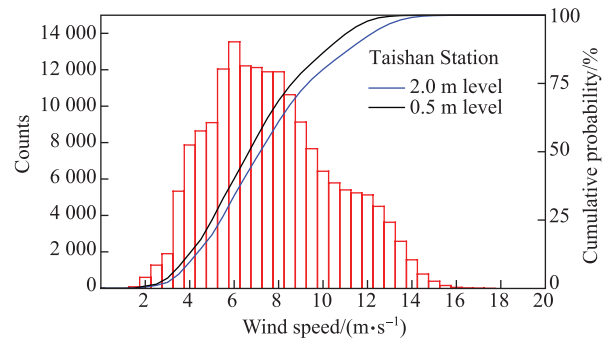
Measurement	Temperature surface/°C	Temperature 0.5 m level/°C	Temperature 2.0 m level/°C	Wind speed 0.5 m level/(m·s <sup>-1</sup> )	Wind speed 2.0 m level/(m·s <sup>-1</sup> )
Max	-13.7	-12.2	-12.2	13.29	14.91
Min	-41.8	-38.4	-38.1	1.55	1.68
Mean	-24.5	-22.2	-22.1	7.14	7.73
25th percentile	-29.0	-26.1	-26.1	5.00	5.39
50th percentile	-24.4	-22.1	-22.0	6.67	7.17
75th percentile	-26.1	-18.5	-18.5	8.60	9.32

at the lower level were weaker than at the high level. Mean, minimum and maximum wind speed differences between the two levels were 0.6, 0.1 and 1.6 m·s<sup>-1</sup>, respectively. Figure 5 gives a histogram of wind speed at 2.0 m. Also shown are the cumulative distributions of speeds at 2.0 m and 0.5 m. The 25th, 50th and 75th percentiles of the 2.0-m speed were 5.39, 7.17 and 9.32 m·s<sup>-1</sup>, respectively. Corresponding measurements at 0.5 m are summarized in Table 1. Daily variations of relative humidity at the two levels and Taishan Station air pressure are plotted in Figures 6 and 7.

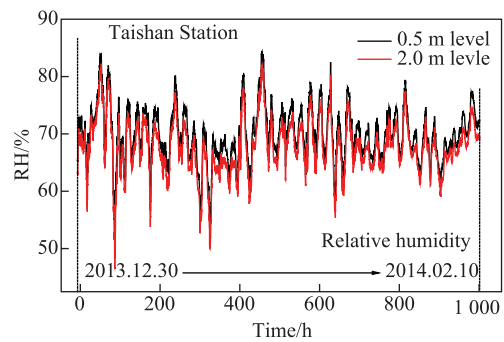
$C_n^2$  at Taishan Station was measured independently by the micro-thermal sensors and CSAT3. Typical  $C_n^2$  measurements from January 11–14, 2014 are shown in Figure 8.  $C_n^2$  shapes from the two sensors are consistent, but their magnitudes frequently deviate, especially for weak turbulence. This contrasts with the situation at Shanghai, China during performance testing of the apparatus, which indicated good agreement of both shapes and the magnitudes, at least for strong turbulence<sup>[20]</sup>. According to Eq. (5), the disagreement between the two methods might be related to the multiscale spatiotemporal turbulence structure and turbulence spectrum at Taishan Station, as well as to applicability of the Taylor assumption<sup>[24]</sup>. In addition, the CSAT3 might have vibrated because of strong wind at the station, which would have altered the transmission distance of the ultrasonic signals. Therefore, the wind could bias the measurement results according to Eq. (5). The data from CSAT3 need further analysis, and results will be reported in a subsequent paper.



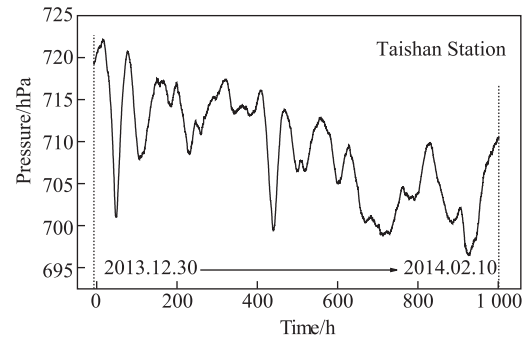
**Figure 4** Measured 0.5-m and 2.0-m wind speeds at Taishan Station in summer, from 05103V and CSAT3 sensors.



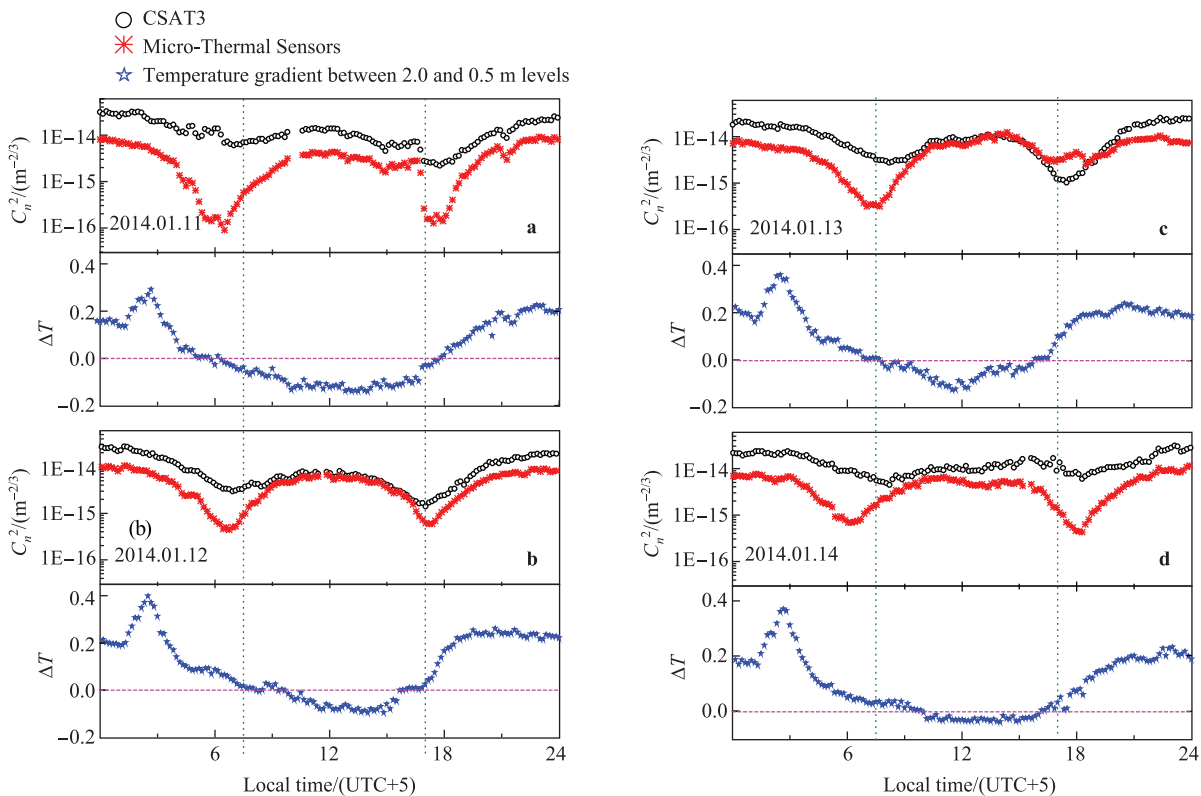
**Figure 5** Histogram of Taishan Station wind speed at 2.0-m height, and cumulative distributions of wind speeds at 2.0-m and 0.5-m heights.



**Figure 6** Measured relative humidity at Taishan Station in summer at 0.5-m and 2.0-m heights.



**Figure 7** Atmospheric pressure measured at Taishan Station.



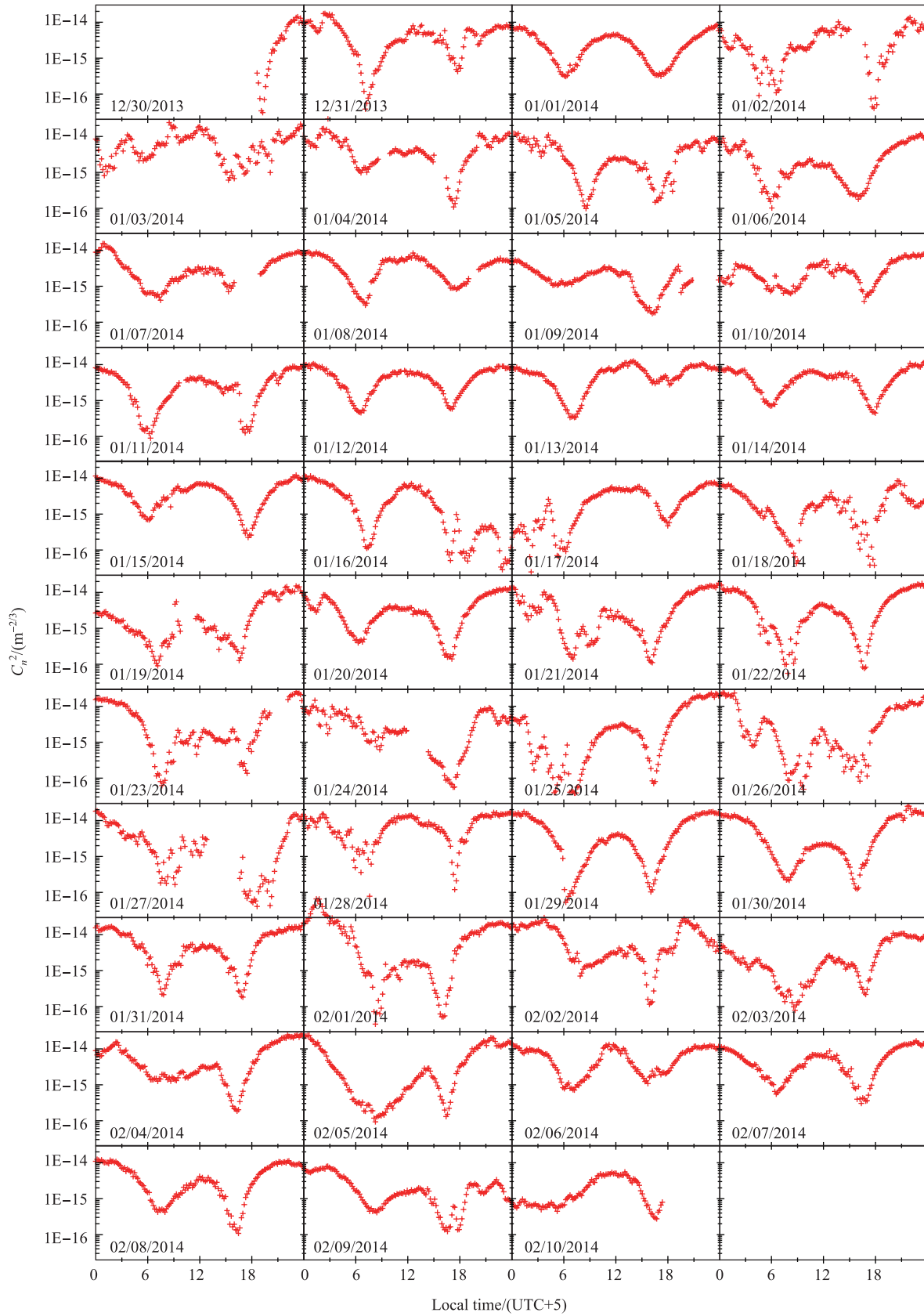
**Figure 8** Comparison of typical  $C_n^2$  measured by micro-thermal sensors and CSAT3 during January 11–14, 2014. Also included in the figure are temperature gradients between heights 2.0 and 0.5 m. Green dotted lines correspond to times at which the minimum  $C_n^2$  normally appeared. There was strong temporal agreement between vanishing of the temperature gradient and the  $C_n^2$  minimum.

Figure 9 shows time series of daily  $C_n^2$  of Taishan Station. We discarded observations when wire of the micro-thermal sensors was broken. The data from 26 d with continuous observation (Figure 9) are averaged in Figure 10. These figures show that  $C_n^2$  had clear structures. There were two peaks around midnight and midday (local time), respectively, and two troughs around 7:30 and 17:00.  $C_n^2$  typically varied over three orders of magnitudes, e.g., from  $10^{-17} \text{ m}^{-2/3}$  to  $10^{-14} \text{ m}^{-2/3}$ . To elucidate the twice-daily minimum of  $C_n^2$ , we present correlation between the daily variation of  $C_n^2$  and temperature gradients at the two heights (0.5 and 2.0 m) in Figure 8. Temperature inversions were observed at night and negative temperature gradients during daytime. There was strong temporal coincidence between vanishing of the temperature gradient and the minimum  $C_n^2$ . Then, the decline of  $C_n^2$  was speculatively put down to the minimum of temperature gradient in this period, resulting in extreme atmospheric stability. The twice-daily maximum of  $C_n^2$  might have resulted from the temperature gradient maximum in this period, giving rise to atmospheric instability. There were no apparent relationships between  $C_n^2$ , relative humidity, wind speed and temperature.

A histogram of  $C_n^2$  measurements is shown in Figure 11. The mean and median  $C_n^2$  were  $4.7 \times 10^{-15} \text{ m}^{-2/3}$  and  $2.8 \times 10^{-15} \text{ m}^{-2/3}$ , respectively. The 25th and 75th percentiles of  $C_n^2$  were  $9.6 \times 10^{-16} \text{ m}^{-2/3}$  and  $6.2 \times 10^{-15} \text{ m}^{-2/3}$ .

## 4 Conclusions

Atmospheric optical turbulence at Taishan Station was measured for the first time using micro-thermal sensors and 3D sonic anemometer at height 2.0 m, from 30 December 2013 to 10 February 2014 during the 30th CHINARE. About 1 000 h of data were obtained. Although  $C_n^2$  shapes from the two sensors agreed well, their magnitudes normally disagreed, which indicates the need for further data analysis. The  $C_n^2$  distribution, measured by the micro-thermal sensors with high resolution, exhibits clear structures with two peaks around midnight and midday (local time), respectively, and two troughs around 7:30 and 17:00. Mean and median values of  $C_n^2$  were  $4.7 \times 10^{-15} \text{ m}^{-2/3}$  and  $2.8 \times 10^{-15} \text{ m}^{-2/3}$ , respectively, and the 25th and 75th percentiles were  $9.6 \times 10^{-16} \text{ m}^{-2/3}$  and  $6.2 \times 10^{-15} \text{ m}^{-2/3}$ . We also acquired meteorological parameters such as temperature, relative humidity, wind speed and air pressure. The site testing data at Taishan Station will furnish key information for astronomical activities. The apparatus was transported to Zhongshan Station to observe atmospheric turbulence in winter for the first time during the 30th CHINARE. It is also planned to perform similar observations at Kunlun Station during the 31st CHINARE. A new instrument equipped with multi-level micro-thermal sensors has been designed, which will be used to observe ground-surface seeing at Taishan Station in the near future.



**Figure 9** Time series of Taishan Station  $C_n^2$  at 2.0-m height from 30 December 2013 to 10 February 2014. Data were measured by micro-thermal sensors.

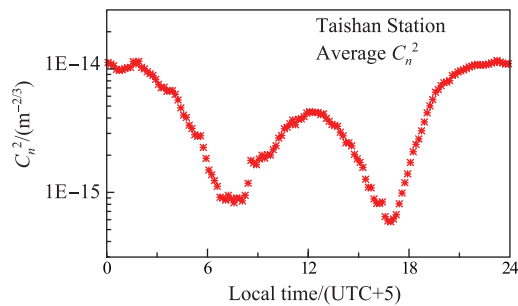


**Figure 10** Time series of average  $C_n^2$  on 26 d at Taishan Station, from continuous observation by micro-thermal sensors.

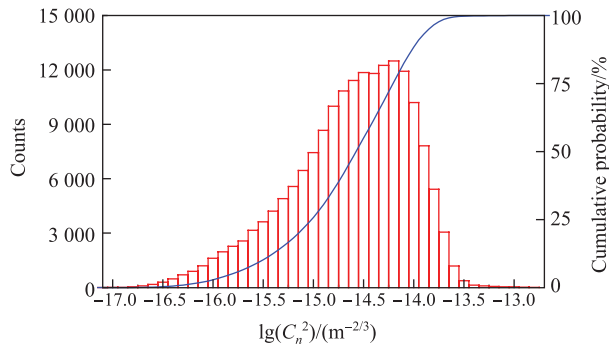


**Figure 11** Histogram and cumulative histogram (solid line) for Taishan Station from 30 December 2013 to 10 February 2014, from micro-thermal sensors at 2.0 m height.

**Acknowledgments** This work was jointly supported by the Chinese Polar Environment Comprehensive Investigation & Assessment Programs (Grant nos. CHINARE-2013-02-03 and CHINARE-2014-02-03), the Polar Science Innovation Fund for Young Scientists of Polar Research Institute of China (Grant no. CX20130201), the Shanghai Natural Science Foundation (Grant no. 14ZR1444100), and the National Basic Research Program of China (973 Program, Grant no. 2013CB834905). The authors gratefully acknowledge Research Fellow Yuan Xiangyan from Nanjing Institute of Astronomical Optics & Technology for meaningful discussions, the engineer Zou Zhengding from the Polar Research Institute of China for carrying out the observations at Taishan Station, and the Polar Research Institute of China for providing excellent logistic support.

## References

- Burton M G. Astronomy in Antarctica. *Astron Astrophys Rev*, 2010, 18(4): 417-469
- Burton M G, Lawrence J S, Ashley M C B, et al. Science programs for a 2-m class telescope at Dome C, Antarctica: PILOT, the Pathfinder for an International Large Optical Telescope. *Publ Astron Soc Austr*, 2005, 22(3): 199-235
- Ashley M C B, Burton M G, Storey J W V, et al. South Pole observations of the near-infrared sky brightness. *Publ Astron Soc Pac*, 1996, 108(726): 721-723
- Nguyen H T, Rauscher B J, Severson S A, et al. The South Pole near-infrared sky brightness. *Publ Astron Soc Pac*, 1996, 108: 718-720
- Phillips A, Burton M G, Ashley M C B, et al. The near-infrared sky emission at the South Pole in winter. *Astrophys J*, 1999, 527(2): 1009-1022
- Marks R D, Vernin J, Azouit M, et al. Antarctic site testing-microthermal measurements of surface-layer seeing at the South Pole. *Astron Astrophys Suppl Ser*, 1996, 118(2): 385-390
- Travouillon T, Ashley M C B, Burton M G, et al. Atmospheric turbulence at the South Pole and its implications for astronomy. *Astron Astrophys*, 2003, 400(3): 1163-1172
- Travouillon T, Ashley M C B, Burton M G, et al. Automated Shack-Hartmann seeing measurements at the South Pole. *Astron Astrophys*, 2003, 409(3): 1169-1173
- Marks R D. Astronomical seeing from the summits of the Antarctic plateau. *Astron Astrophys*, 2002, 385: 328-336
- Marks R D, Vernin J, Azouit M, et al. Measurement of optical seeing on the high Antarctic plateau. *Astron Astrophys Suppl Ser*, 1999, 134: 161-172
- Lawrence J S, Ashley M C B, Tokovinin A, et al. Exceptional astronomical seeing conditions above Dome C in Antarctica. *Nature*, 2004, 431(7006): 278-281
- Agabi A, Aristidi E, Azouit M, et al. First whole atmosphere nighttime seeing measurements at Dome C, Antarctica. *Publ Astron Soc Pac*, 2006, 118(840): 344-348
- Aristidi E, Fossat E, Agabi A, et al. Dome C site testing: surface layer, free atmosphere seeing, and isoplanatic angle statistics. *Astron Astrophys*, 2009, 499(3): 955-965
- Walden V P, Town M S, Halter B, et al. First measurements of the infrared sky brightness at Dome C, Antarctica. *Publ Astron Soc Pac*, 2005, 117(829): 300-308
- Yang H, Allen G, Ashley M C B, et al. The PLATO Dome A site-testing observatory: Instrumentation and first results. *Publ Astron Soc Pac*, 2009, 121(876): 174-184
- Lawrence J S, Ashley M C B, Hengst S, et al. The PLATO Dome A site-testing observatory: Power generation and control systems. *Rev Sci Instrum*, 2009, 80(6): 064501-1-10
- Bonner C S, Ashley M C B, Cui X, et al. Thickness of the atmospheric boundary layer above Dome A, Antarctica, during 2009. *Publ Astron Soc Pac*, 2010, 122(895): 1122-1131
- Okita H, Ichikawa T, Ashley M C B, et al. Excellent daytime seeing at Dome Fuji on the Antarctic plateau. *Astron Astrophys Lett*, 2013, 554: L5
- Wu X Q, Qian X M, Huang H H, et al. Measurements of Seeing, isoplanatic angle, and coherence time by using balloon-borne microthermal probes in Gaomeigu. *Acta Astronomica Sinica*, 2014, 55(2): 144-153 (in Chinese with English abstract)
- Tian Q G, Chai B, Wu X Q, et al. A mobile polar atmospheric parameter measurement system: I. development and performance testing. *Chinese J of Polar Res*, 2015, 27(2): 125-131 (in Chinese with English abstract)
- Tatarskii V I. Wave propagation in a turbulent medium. New York: McGraw-HILL BOOK Company, INC., 1961
- Campbell Scientific, Inc. CSAT3 three dimensional sonic anemometer instruction manual. Logan, Utah: Campbell Scientific, Inc., 2012
- Zhu X T, Wu X Q, Li D Y. Characteristics of ASL turbulence spectra and  $C_n^2$  using three-dimensional ultrasonic anemometer. *J Atmos and Environ Opt*, 2012, 7(1): 6-12 (in Chinese with English abstract)
- Nichols-Pagel G A, Percival D B, Reinhall P G, et al. Should structure functions be used to estimate power laws in turbulence? A comparative study. *Phys D: Nonl Phen*, 2008, 237(5): 665-677